


CLINICAL REPORT

Clinical and genetic characterization of three Russian patients with pycnodysostosis due to pathogenic variants in the *CTSK* gene

Tatiana Vladimirovna Markova¹  | Vladimir Kenis² | Evgeniy Melchenko² |
Darya Guseva¹ | Darya Osipova¹  | Nailya Galeeva¹ | Tatiana Nagornova¹ |
Elena Leonidovna Dadali¹

¹Research Centre for Medical Genetics, Moscow, Russia

²H. Turner National Medical Research Center for Children's Orthopedics and Trauma Surgery, Pushkin, Russia

Correspondence

Markova Tatiana Vladimirovna, Genetic counselling, Research Centre for Medical Genetics, Moskvorechye st., 1, Moscow 115522, Russia.
Email: markova@med-gen.ru

Abstract

Background: Pycnodysostosis (PD, OMIM # 265800) is a rare variant of skeletal dysplasia with an autosomal recessive type of inheritance, characterized by a combination of specific features such as disproportionate nanism, generalized osteosclerosis, and distinct craniofacial dysmorphism. Radiographic features include acro-osteolysis of the distal phalanges in association with sclerosing bone lesions with multiple fractures. The polymorphism of the clinical manifestations of pycnodysostosis and low prevalence of the disorder lead to the difficulties with early.

Methods: The following tests were used for diagnostics: genealogical analysis, clinical examination, neurological examination according to the standard method with an assessment of the psychoemotional sphere, radiological analysis, searching for pathogenic variants in the *CTSK* gene by the automated Sanger sequencing.

Results: We describe first clinical and genetic characteristics of three Russian patients with pycnodysostosis from unrelated families. Two patients have a novel homozygous nucleotide substitution c.746T>A (p. Ile249Asn), and one has a previously described homozygous pathogenic variant c.746T>C (p. Ile249Thr) in the *CTSK* gene. In all three cases, a transition or transversion was found at nucleotide position 746 in exon 6 of the *CTSK* gene, leading to two different amino acid substitutions in the polypeptide chain. The obtained results may indicate the presence of a major pathogenic variant in the *CTSK* gene, leading to the typical manifestation of the disease.

Conclusion: The data presented in the study enlarge the clinical, radiological, and mutational spectrum of pycnodysostosis. Typical clinical manifestations and the small size of the *CTSK* gene make the automated Sanger sequencing the optimal method for diagnosis of pycnodysostosis.

This is an open access article under the terms of the Creative Commons Attribution-NonCommercial-NoDerivs License, which permits use and distribution in any medium, provided the original work is properly cited, the use is non-commercial and no modifications or adaptations are made.

© 2022 The Authors. *Molecular Genetics & Genomic Medicine* published by Wiley Periodicals LLC.

KEYWORDS

CTSK gene, pycnodysostosis, skeletal dysplasia

1 | INTRODUCTION

Pycnodysostosis (PD; OMIM # 265800) is a rare skeletal dysplasia with an autosomal recessive type of inheritance. The first description of the disease was made by Maroteaux and Lamy (1962). This condition got its name due to the presence of a specific x-ray sign, which is characterized by an increase in bone density resulting from osteoclast dysfunction and the development of generalized osteosclerosis (from Greek «pycnos» means «dense»). Its prevalence is 1–3 per 1,000,000 people (Araujo et al., 2016; Xue et al., 2011). Consanguinity of patient's parents was confirmed in 30%–81% of families in certain populations (Bizaoui et al., 2019; Sedano et al., 1968).

Typical clinical signs of the disease include short stature (on average -3.5 SD), hypoplastic midface, beaked nose, micrognathia, high palate, crowded carious teeth, frontal and occipital prominence, substantially delayed closure of the fontanelles and sutures, short wide distal phalanges of the fingers and toes, dysplastic nails and predisposition to spontaneous fractures with delayed healing (Arman et al., 2014; Bizaoui et al., 2019; Sedano et al., 1968; Xue et al., 2011). Skeletal radiographs typically demonstrate diffuse osteosclerosis increasing with the child's growth, opened skull sutures and fontanelles, and the wormian bones. In most cases, there is an obtuse angle of the mandible, hypopneumatization of the paranasal sinuses and mastoid process, hypoplasia of the acromial end of clavicle and acro-osteolysis of the distal phalanges (Arman et al., 2014; Bizaoui et al., 2019; Sedano et al., 1968; Xue et al., 2011). Characteristic features also include delayed eruption of permanent teeth and persistence of deciduous teeth (Alves & Cantín, 2014).

In 1995 Polymeropoulos et al. mapped the candidate of pycnodysostosis gene locus on chromosome 1q21 and in 1996 Gelb et al. identified pathogenic variants in the *CTSK* gene (Gelb et al., 1995; Polymeropoulos et al., 1995). Cathepsin K (*CTSK*; OMIM # 601105) is a gene product, from the group of lysosomal cysteine proteases which expressed predominantly in osteoclasts and involved in the degradation of bone matrix proteins (Gelb, Moissoglu, et al., 1996). It has been shown that insufficient bone resorption by osteoclasts, especially type I collagen, which forms 95% of the organic bone matrix, causes diffuse osteosclerosis, and bone fragility (Gelb, Moissoglu, et al., 1996).

The polymorphism of the PD clinical manifestations and its low prevalence make it difficult to have an accurate diagnosis early. Sometimes the diagnosis is made late

after atypical bone fractures, in some cases the disease is misinterpreted as one of the types of osteopetrosis or cleidocranial dysplasia (Bizaoui et al., 2019; Xue et al., 2011).

To date, 64 pathogenic variants, leading to polymorphic clinical manifestations of PD have been identified in the *CTSK* gene (Stenson et al., 2003). However, the lack of detailed clinical data in the literature makes the clinical and genetic correlation difficult (Arman et al., 2014; Bizaoui et al., 2019). Therefore, it is important to describe the clinical features and radiological signs in patients with both previously identified and newly identified variants of the *CTSK* gene, which will contribute not only to predicting the severity of the disease, but also to improve the understanding of the underlying mechanisms of the pathology.

2 | MATERIALS AND METHODS

A comprehensive complex examination of three children from unrelated families (one girl aged 11 years old and two boys aged 13 years and 2 years old) with phenotypic signs of skeletal dysplasia was carried out at Research Center for Medical Genetics, Moscow. To determine the diagnosis, following medical tests were used: genealogical analysis, clinical examination, neurological examination according to the standard method with an assessment of the psychoemotional sphere, x-ray analysis, searching for pathogenic variants in the *CTSK* gene by the automated Sanger sequencing. WHO growth charts were used to describe SD growth parameters in probands (The WHO Child Growth Standards, n.d.).

2.1 | Genetic analysis

Genomic DNA samples isolated from whole blood samples using a Wizard® Genomic DNA Purification Kit (Promega, USA) according to the manufacturer's protocol were used. Searching for pathogenic variants in the *CTSK* gene was performed by automated Sanger sequencing. RefSeqGene accession numbers NM_000396.4 and NP_000387.1 for the *CTSK* gene were used. The primer sequences, MgCl₂ concentration, and primer annealing temperature are presented in (Table 1). To analyze the electrophoretic mobility of the amplified fragments, a 7% gel with an acrylamide: bisacrylamide ratio of 29:1 was used. PCR products were sequenced using the ABI PRISM BigDye Terminator (v 3.1) Cycle Sequencing Kit (Applied

TABLE 1 Primers and conditions for PCR of DNA fragments performing, containing the coding regions of the *CTSK* gene

DNA fragment	Primer's sequence	Fragment's length, bp	Concentration MgCl ₂ , mM	Annealing temperature of primers, °C (number of cycles)
Exon 1	F-GACAGTCTTGTGAGACTAAATAGC R-GCTTTTCATTCTGTCAATTCTCTG	326	2	63 (31)
Exon 2	F-GCCTAGTTTTCCTCTGTTTCCC R-GCATGGCAGGAAGGCTGAGAC	226	2	63 (31)
Exons 3–4	F-CATATGTAAGTGTAGACAGTCTATAC R-GTGCATATGAATCTGGCATGAC	458	2	63 (31)
Exon 5	F-CTTCAGGCAGGTAGAGAGAAGA R-GCTCTGTTGGCTCCTCCTTCC	338	2	63 (31)
Exons 6–7	F-CTCATTGCCTATTGCTTTGTCC R-GTCACCCTTTTAACTCAACC	645	2	63 (31)
Exon 8	F-CATCAGTACCTCGACAATACTC R-GCTCTTCCATTCTTCCACGATG	233	2	63 (31)

Biosystems) on an ABI3130xl Genetic Analyzer (Applied Biosystems). The sequencing results were analyzed using the BLAST program (<http://www.ncbi.nlm.nih.gov/blast>).

3 | RESULTS

3.1 | Patient 1

A female proband was presented at the age of 11 years old. The child had short stature and the history of the fractures of the lower limbs. The parent's marriage is consanguineous. They are cousins of Tatar nationality living on the territory of the Tatarstan (central part of Russian Federation). The child was born from the first pregnancy with timely delivery: body weight of 2900 g (−0.75 SD), length of 48 cm (−0.62 SD) with an Apgar score of 8/9 points.

At the age of 3 months, she was diagnosed with bilateral hip dysplasia which was treated conservatively with positive result at the age of 1 year, nevertheless residual dysplasia of the left hip was noticed later. Enlarged anterior fontanelle was noticed since neonatal period and at the age of 1 year the width of the fontanelle was 2.5 × 2.5 cm. During early childhood she demonstrated low muscle tone, motor delay (independent walking was achieved after she was 2 years old). She was referred to pediatric endocrinologist because of the short stature. Normal karyotype 46, XX was confirmed, after that she was suspected with skeletal dysplasia (hypochondroplasia). Orthopedic surveillance revealed residual dysplasia of the left hip and surgical treatment was recommended. Head MRI and CT revealed relative thickening of the optical nerves, reduced volume of posterior fossa with elongated shape of the occipital bone, narrowing of the foramen magnum, and

mild Arnold-Chiari malformation. She was also referred to ophthalmologist because of visual impairment, where partial atrophy of the optic discs and mild hypermetropia were found.

Radiographs of both hands performed at the age of 5 years demonstrated complex brachydactyly with evident sign of acro-osteolysis of the 1–3 digits distal phalanges, shortening and deformity of the second and fifth digits middle phalanges. From the age of 8.5 years repeated low-energy fractures of both tibiae with delayed formation and high density callus occurred.

At the age of 11 years her height was 113 cm (−4.82 SD), body mass was 21 kg (−3.7 SD), BMI was 16.45 (−0.39 SD), head circumference was 50 cm (−2.5 SD). Dysmorphic features included prominent forehead, gray-blue sclerae, bulbous nose, micrognathia, crowded teeth, multiple caries. Among other clinical features brachydactyly with broadening of the distal phalanges of hands and feet, skin wrinkles on the dorsal part of the fingers, broad and short nails with transverse stripes, hypermobility of the interphalangeal and metacarpophalangeal joints, mild deficit of elbow extension were noticed. Orthopedic manifestations included thoracolumbar scoliosis, lumbar hyperlordosis, valgus knees, and plano-valgus feet.

Radiographs revealed increased cortical bone density, mild undertubulation of the distal metaphyses of the tibia and radius, fracture of the midshaft of the tibia with cortical thickening, osteolysis of the ends of the distal phalanges, fractures of the metatarsal bones (Figure 1).

Based on clinical and radiological data, it was assumed that the child had PD. The diagnosis was confirmed with the *CTSK* gene analysis by automated Sanger sequencing, where was revealed the previously described pathogenic variant in exon 6: c.746T>C (p.Ile249Thr) in a homozygous state. Parents were heterozygous for this variant.



FIGURE 1 Clinical and radiological features of first patient. (a) Outer appearance of the hands. (b) Outer appearance of the feet. (c) AP radiograph of the left calf: Mild undertubulation of the distal metaphysis of the tibia (white arrow); healing fracture of the midshaft of the tibia with cortical thickening (black arrow). (d) AP radiograph of the pelvis and hips demonstrates dysplastic left hip with increased acetabular angle, increased neck-shaft angle, decreased acetabular coverage of the femoral head (white circle), increased bone density in the supraacetabular areas (white arrows), thickening of the cortical layers of pubic bones (white arrowheads), thickening of the inner (black arrows), and outer (red arrows) cortical bone of the proximal femur. (e) AP radiograph of the hand: osteolysis of the distal ends of the distal phalanges (red arrows); pseudoepiphyses of the metacarpals (white arrows); undertubulation of the distal metaphysis of the radius (black arrow). (f) AP radiograph of the foot: osteolysis of the distal ends of the distal phalanges of the toes (red arrows); healing fracture of the second and third metatarsal (white arrows); healed fracture of the fourth metatarsal (black arrow)

3.2 | Patient 2

A male proband was examined at the age of 13 years old due to short stature. The child's parents are healthy and not consanguineous. Family members by nationality are Avars and live in the territory of the Dagestan Republic (Northern Caucasus, Russian Federation). The family also has four healthy children: the elder brother of the proband is 16 years old and the younger brothers are 11, 10 years old, and 1 year old. The proband was born from second timely delivery with body weight of 3500 g (0.31 SD), length of 53 cm (1.65 SD). Pregnancy proceeded with polyhydramnios.

During the first year of life, a CT scan of the brain was performed, where were found mixed hydrocephalus and opened fontanelles. Psychomotor development proceeded according to the age. Proband achieved the head control from 3 months, independent sitting from 7 months, walking independently from 1 year old. From the age of 5, due to growth retardation, he was receiving growth hormone therapy for 3 years.

First fracture of the left tibia was diagnosed at the age of 7.5 years. Then almost annually metatarsal fractures on both feet were detected. Radiographs of the skull performed at the age of 11 years revealed dense cranial bones, sclerosis of the skull base, wide sutures, opened fontanelle. On the radiographs of the hands at the same age complex brachydactyly with acro-osteolysis were noticed. Brain MRI did not reveal any anatomical abnormalities. He was suspected with Hajdu-Cheney syndrome and genetic testing was recommended.

At the age of 13 years disproportionally short stature with predominant shortening of the hands and feet, brachydactyly, hypermobility of the interphalangeal joints, shortening of the distal phalanges, hypoplastic nails were noticed. Body height was 140 cm (−2.16 SD), body mass was 57 kg (2.5 SD), BMI was 29 (2.65 SD), and head circumference was 55 cm (0.9 SD). Among orthopedic manifestation mild thoracolumbar scoliosis, plano-valgus feet were diagnosed. Other dysmorphic features included brachycephaly, opened fontanelle (0.5 × 0.3 cm), gray-blue sclerae, elongated nose with hypoplastic alae, high palate, retro-, and micrognathia, crowded teeth (Figure 2).

Radiographs revealed increased bone density of pelvic bones and proximal femur, undertubulation of the long tubular bones (more prominent in the distal metaphyses of the distal femora and tibiae. Radiographs of the hands demonstrated acro-osteolysis (osteolysis of the distal ends of the distal phalanges), narrowing of the diaphyses of the middle and basal phalanges. Radiographs of the feet also showed acro-osteolysis and healing fracture of the metatarsals.

The combination of clinical and radiological findings suggested the PD presence in the child. The diagnosis was confirmed with *CTSK* gene analysis by automated Sanger sequencing, which detected a novel variant in exon 6: c.746T>A (p.Ile249Asn) in a homozygous state. This variant frequency in the GnomAD database is 0.000657%. Pathogenicity prediction algorithms consider this variant as pathogenic: SIFT, PolyPhen2_HDIV, PolyPhen2_HVAR, MetaLR, MetaSVM, MetaRNN, REVEL, BayesDel addAF, BayesDel noAF, DEOGEN2, EIGEN, FATHMM, LRT, M-CAP, and MutationTaster. This variant is located in a highly conservative region: PhyloP100way (score 9.325). Parents were heterozygous for this variant, which made it possible to diagnose PD in the patient.

3.3 | Patient 3

A male proband from the Chechen family was examined at the age of 2 years and 8 months, due to short stature, opened fontanelles, and delayed cranial sutures closure. The child's parents are four-generation cousins living in the territory of the Chechen Republic (Northern Caucasus, Russian Federation). The child was born from the first pregnancy, at term with body weight of 3250 g (−0.2 SD), length of 49 cm (−0.47 SD), and Apgar score of 8/9 points. The proband has begun walking and speaking separate words since 1 year and 3 months old. There was a delayed eruption of deciduous teeth, as the first tooth appeared at the age of 1 year. The patient was followed by a pediatrician from the age of 4 months due to delay in physical development. MRI examination of the brain at the age of 1 year revealed signs of moderate internal hydrocephalus. The ophthalmologist diagnosed hyperopic astigmatism in both eyes.

Radiography at the age of 2 years and 3 months revealed hypoplastic sternal ends of the clavicles, pseudoepiphyses of the metacarpal bones, delayed bone age (15–18 months). He was suspected to have cleidocranial dysostosis.

At the age of 2 years and 8 months, his height was 84 cm (−2.53 SD), weight was 10 kg (−2.27 SD), BMI was 19.6 (−0.85 SD), and head circumference was 49.5 cm (0.93 SD). Among the characteristic dysplastic features prominent forehead and parietal tuber of the skull, enlarged fontanelle (5x5 cm), opened fissures and posterior fontanelle, gray-blue sclerae, elongated nose with upturned tip, micrognathia, narrow shoulders were noticed. Brachydactyly of the hands and feet, hypoplastic nails with transverse striping were also remarked.

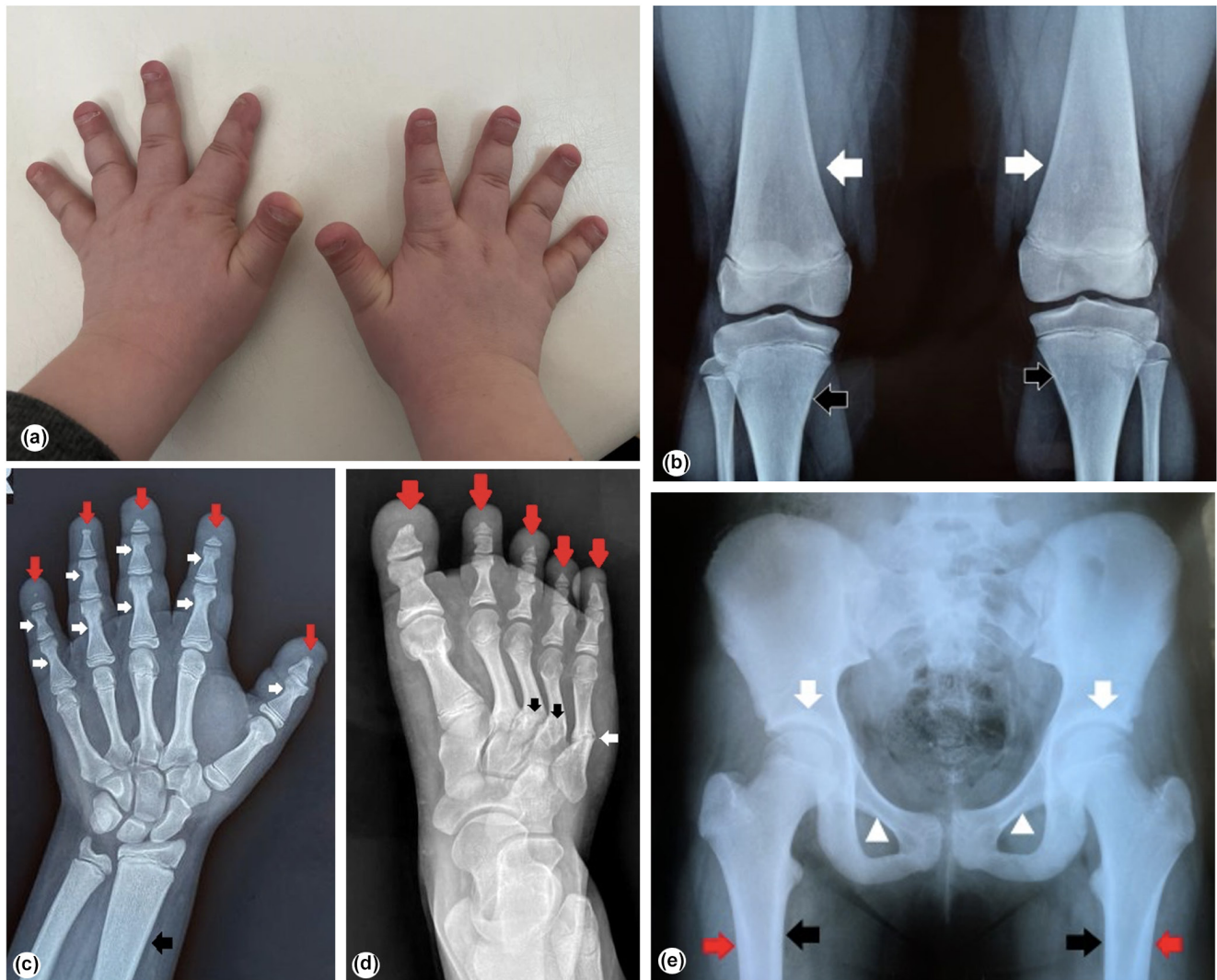


FIGURE 2 Clinical and radiological features of second patient. (a) Outer appearance of the hands. (b) AP radiographs of the both knee joints: Undertubulation of the distal metaphyses of the femora (white arrows) and proximal tibiae (black arrows). (c) AP radiograph of the hand: Osteolysis of the distal ends of the distal phalanges (red arrows); narrowing of the diaphyses of the middle and basal phalanges (white arrows); undertubulation of the distal metaphysis of the radius (black arrow). (d) AP radiograph of the foot: Osteolysis of the distal ends of the distal phalanges of the toes (red arrows); healing fracture of the fifth metatarsal (white arrow); healed fractures of fourth and third metatarsals (black arrows). (e) AP radiograph of the pelvis and hips demonstrates normal hip joints, increased bone density in the supraacetabular areas (white arrows), thickening of the cortical layers of pubic bones (white arrowheads), thickening of the inner (black arrows), and outer (red arrows) cortical bone of the proximal femur

Radiographs of the skull revealed diffuse osteosclerosis, opened fontanelle, delayed suture closure, and obtuse angle to mandible. Among other radiological features dense cortical layer of the pelvic and femoral bones, hypoplastic clavicles, short distal phalanges with acroosteolysis were revealed (Figure 3).

Clinical and radiological data made it possible to suspect PD in the proband. Analysis of the *CTSK* gene by automated Sanger sequencing revealed a novel variant in exon 6: c.746T>A (p.Ile249Asn) in a homozygous state. Parents were heterozygous for this variant, which made it possible to diagnose PD in the proband.

4 | DISCUSSION

PD refers to primary sclerosing dysplasias of the skeleton, characterized by short stature, specific dysmorphic facial features, and susceptibility to spontaneous fractures. In the international classification of hereditary skeletal diseases PD is classified into one group with osteopetrosis, which also cause generalized osteosclerosis (Mortier et al., 2019). The similar clinical manifestations of these two conditions require early differential diagnosis due to the different approaches to their treatment, using molecular genetic methods.

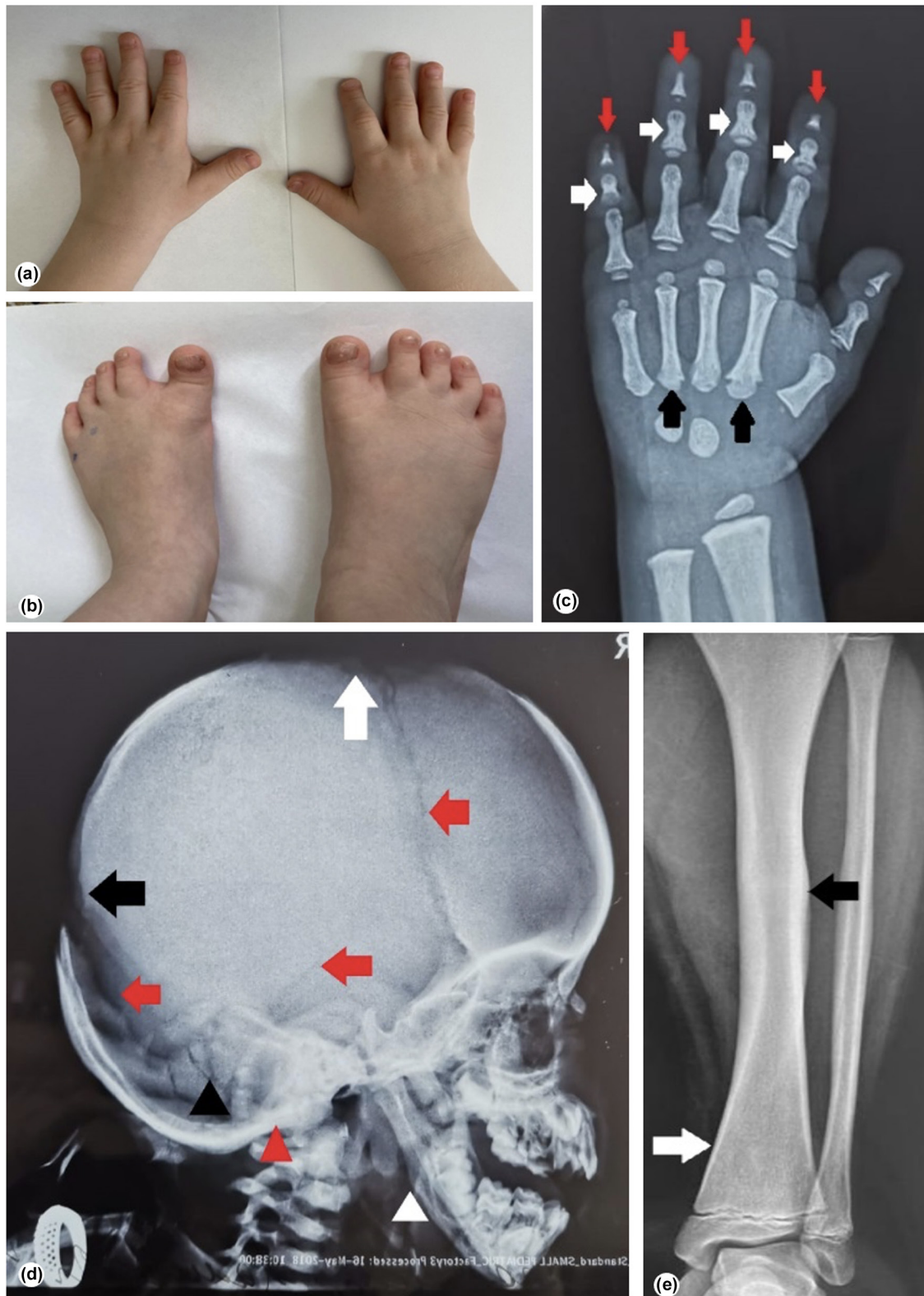


FIGURE 3 Clinical and radiological features of third patient. (a) Outer appearance of the hands. (b) Outer appearance of the feet. (c) AP radiograph of the hand: Osteolysis of the distal ends of the distal phalanges (red arrows); narrowing of the diaphyses of the middle and basal phalanges (white arrows); pseudoepiphyses of the metacarpals (black arrows). (d) Lateral radiograph of the skull: Opened anterior (white arrow) and posterior (black arrow) fontanelles; opened sutures (red arrows); wormian bones (black arrowhead); dense bones of the skull base (red arrowhead); obtuse mandibular angle (white arrowhead). (e) AP radiograph of the left calf: Undertubulation of the distal metaphysis of the tibia (white arrow); healed fracture of the midshaft of the tibia with cortical thickening (black arrow)

It has been shown that early transplantation of hematopoietic stem cells can be a targeted treatment option for some forms of osteopetrosis but not for pycnodysostosis, which is characterized by the preservation of the medullary cavity in long tubular bones with normal hematopoietic function (Ihde et al., 2011). It is necessary to make a differential diagnosis of PD with several hereditary diseases. The first signs of the disease which can draw attention of the pediatricians are disproportionate dwarfism and delayed closure of the fontanelles. The combination of these features with clavicle hypoplasia was the reason for the preliminary diagnosis of cleidocranial dysplasia in patient 3 in early childhood, before the bone fractures occurred.

However, the anomaly of the clavicles (up to the total absence) is more severe in patients with cleidocranial dysplasia. At the same time, these patients do not demonstrate the combination of increased bone density and acroosteolysis, which is typical for PD (Schmidt et al., 2020; Xue et al., 2011). Acro-osteolysis caused the misdiagnosis of Hajdu-Cheney syndrome in patient 2. Therefore, it is important to focus on generalized osteoporosis, which is typical for Hajdu-Cheney disease and absent in PD (Simpson et al., 2011). Disproportionate dwarfism in combination with macrocephaly and brachydactyly were the reason for misdiagnosis of hypochondroplasia in patient 1. Assessment of phenotypic features in PD patients plays a significant role in the differential diagnosis of these diseases, taking into consideration that PD is characterized by: micrognathia (95%), beaked nose (67%), proptosis (60%), gray-blue sclerae (40%), and crowded teeth (67%) (Bizaoui et al., 2019).

Distinctive symptoms of PD are hypoplasia of the facial bones and mandible, which lead the risk of obstructive sleep apnea requiring polysomnography (Bizaoui et al., 2019). The predisposition to the fractures of the tubular bones in the older age is a key-specific feature of PD, which is important for its diagnosis. According to the study by Bizaoui et al. (2019), first bone fractures in patients with PD most often occur at the age of 7–10 years and characterized by slow healing (Bizaoui et al., 2019). The first fractures in patients 1 and 2 were registered at the age of 8.5 and 7.5 years, respectively. The PD diagnosis in probands led to discontinuation of bisphosphonate therapy in patient 1, which is contraindicated in this condition. It is known that the *CTSK* gene, which is responsible for the PD development, contains 12,000 base pairs and consists of eight exons (Bizaoui et al., 2019; Xue et al., 2011). To date, 64 pathogenic variants in the *CTSK* gene have been described that lead to the PD development. The majority of pathogenic variants are missense substitutions (73%), most of them are localized in the “hot” spots of exons 6 and 7 (Stenson et al., 2003).

The protein product of the *CTSK* gene consists of 329 amino acids and includes a preroion (15 amino acids), a proregion (99 amino acids), and a mature active enzyme (215 amino acids) (Donnarumma et al., 2007). Cathepsin K is synthesized as a proenzyme before being transported to lysosomes, where it is cleaved to an active enzyme form at low pH as a result of the autocatalytic process of removing the N-terminal region (McQueney et al., 1997). It has been shown that 69.7% of pathogenic variants were identified in the mature domain, 24.24% in the proregion and 6.06% in the preroion of the protein (Xue et al., 2011).

Interestingly, that two of our patients of different nationalities have a previously undescribed transversion c.746T>A (p.Ile249Asn) in a homozygous state in exon 6 of the *CTSK* gene, which leads to the substitution of isoleucine to asparagine at 249 position of the amino acid sequence. The patients came from two unrelated families and belonged to different nationalities—Avars and Chechens, and only one family was consanguineous. In one patient, a homozygous substitution of thymine in the same position to cytosine 746T>C (p.Ile249Thr) was found, which led to the isoleucine to threonine substitution. This variant was previously described by Donnarumma et al. (2007) in compound heterozygous state in combination with another pathogenic variant in the Spanish family and Huang et al. (2015) found it in a homozygous state in the Chinese patient with PD. Donnarumma et al. (2007), who first described this variant in compound heterozygous state with the nonsense variant p.Arg241X, modeled the three-dimensional structure of cathepsin K and found a hydrophobic cluster important for protein folding, which includes the residue Ile249. Thus, the authors showed that replacing hydrophobic isoleucine with hydrophilic threonine destabilizes this hydrophobic cluster and disrupts the folding and function of cathepsin K. Amino acid substitution, which was first identified in two of our probands, also led to the replacement of hydrophobic isoleucine by hydrophilic asparagine (p.Ile249Asn). It can be assumed that the identified amino acid substitution also disrupts protein folding, causing its functional insufficiency.

Thus, our results in combination with the last literature data indicate that the transition or transversion of the T (thymine) nucleotide at position 746 could be one of the major pathogenic variants in the *CTSK* gene, leading to the PD development. However, this assumption requires further research and data accumulation.

5 | CONCLUSION

Pycnodysostosis is a rare autosomal recessive skeletal dysplasia characterized by a combination of disproportionate dwarfism, generalized osteosclerosis, and specific

craniofacial dysmorphism. Radiographic features include acro-osteolysis of the distal phalanges in association with sclerosing bone lesions with multiple fractures. We observed three Russian patients with PD, two of them had a novel homozygous nucleotide substitution c.746T>A (p.Ile249Asn), and the other one had a previously described homozygous variant c.746T>C (p.Ile249Thr) in *CTSK* gene. There was a 746 nucleotide transition or transversion in exon 6 of the gene in all three cases, that leading to two different amino acid substitutions in the polypeptide chain. At the same time, in both cases, the hydrophobic amino acid was replaced by a hydrophilic one, which, as shown earlier, leads to dysfunction of the gene product. The results may indicate the presence of a major pathogenic variant in the *CTSK* gene, leading to the PD development, however, this assumption requires further research. Criteria for the PD diagnosis and its differential diagnosis are presented. Based on the typical clinical manifestations and small size of the *CTSK* gene, it has been shown that automated Sanger sequencing is the optimal method for diagnosis of PD.

CONFLICT OF INTEREST

The authors declare no conflict of interest.

ETHICAL COMPLIANCE

All research participants gave informed consent to the clinical examination and the publication of their anonymized data. The study was performed in accordance with the Declaration of Helsinki and approved by the Institutional Review Board of the Research Center for Medical Genetics, Russia.

DATA AVAILABILITY STATEMENT

Data available on request due to privacy/ethical restrictions. The novel variant was submitted to the ClinVar database. Variant number is SCV001984978.

ORCID

Tatiana Vladimirovna Markova  <https://orcid.org/0000-0002-2672-6294>

Darya Osipova  <https://orcid.org/0000-0002-5863-3543>

REFERENCES

- Alves, N., & Cantín, M. (2014). Clinical and radiographic maxillofacial features of pycnodysostosis. *International Journal of Clinical and Experimental Medicine*, 7(3), 492.
- Araujo, T. F., Ribeiro, E. M., Arruda, A. P., Moreno, C. A., de Medeiros, P. F. V., Minillo, R. M., Melo, D. G., Kim, C. A., Doriqui, M. J. R., Felix, T. M., Fock, R. A., & Cavalcanti, D. P. (2016). Molecular analysis of the *CTSK* gene in a cohort of 33 Brazilian families with pycnodysostosis from a cluster in a Brazilian northeast region. *European Journal of Medical Research*, 21(1), 1–11. <https://doi.org/10.1186/S40001-016-0228-7>
- Arman, A., Bereket, A., Coker, A., Kiper, P. Ö., Güran, T., Ozkan, B., Atay, Z., Akçay, T., Haliloglu, B., Boduroglu, K., Alanay, Y., & Turan, S. (2014). 'Cathepsin K analysis in a pycnodysostosis cohort: Demographic, genotypic and phenotypic features. *Orphanet journal of rare diseases*, 9(1), 60. <https://doi.org/10.1186/1750-1172-9-60>
- Bizaoui, V., Michot, C., Baujat, G., Amouroux, C., Baron, S., Capri, Y., Cohen-Solal, M., Collet, C., Dieux, A., Geneviève, D., Isidor, B., Monnot, S., Rossi, M., Rothenbuhler, A., Schaefer, E., & Cormier-Daire, V. (2019). Pycnodysostosis: Natural history and management guidelines from 27 French cases and a literature review. *Clinical Genetics*, 96(4), 309–316. <https://doi.org/10.1111/CGE.13591>
- Donnarumma, M., Ribeiro, E. M., Arruda, A. P., Moreno, C. A., de Medeiros, P. F., Minillo, R. M., Melo, D. G., Kim, C., Doriqui, M. J., Felix, T. M., & Fock, R. A. (2007). Molecular analysis and characterization of nine novel *CTSK* mutations in twelve patients affected by pycnodysostosis. *Human Mutation*, 28(5), 524–524. <https://doi.org/10.1002/HUMU.9490>
- Gelb, B. D., Moissoglu, K., Zhang, J., Martignetti, J. A., Brömme, D., & Desnick, R. J. (1996). Cathepsin K: Isolation and characterization of the murine cDNA and genomic sequence, the homologue of the human pycnodysostosis gene. *Biochemical and Molecular Medicine*, 59(2), 200–206. <https://doi.org/10.1006/BMME.1996.0088>
- Gelb, B. D., Shi, G. P., Chapman, H. A., & Desnick, R. J. (1996). Pycnodysostosis, a lysosomal disease caused by cathepsin K deficiency. *Science*, 273(5279), 1236–1239. <https://doi.org/10.1126/SCIENCE.273.5279.1236>
- Gelb, B. D., Edelson, J. G., & Desnick, R. J. (1995). Linkage of pycnodysostosis to chromosome 1q21 by homozygosity mapping. *Nature Genetics*, 10(2), 235–237. <https://doi.org/10.1038/NG0695-235>
- Huang, X., Qi, X., Li, M., Wang, O., Jiang, Y., Xing, X., Hu, Y. Y., & Xia, W. (2015). 'A mutation in *CTSK* gene in an autosomal recessive Pycnodysostosis family of Chinese origin. *Calcified Tissue International*, 96(5), 373–378. <https://doi.org/10.1007/S00223-015-9963-Y>
- Ihde, L. L., Forrester, D. M., Gottsegen, C. J., Masih, S., Patel, D. B., Vachon, L. A., White, E. A., & Matcuk, G. R., Jr. (2011). Sclerosing bone dysplasias: Review and differentiation from other causes of osteosclerosis. *Radiographics*, 31(7), 1865–1882. <https://doi.org/10.1148/RG.317115093>
- Maroteaux, P., & Lamy, M. (1962). Pycnodysostosis. *Presse Médicale*, 25(70), 999–1002.
- McQueney, M. S., Amegadzie, B. Y., D'Alessio, K., Hanning, C. R., McLaughlin, M. M., McNulty, D., Carr, S. A., Ijames, C., Kurdyla, J., & Jones, C. S. (1997). Autocatalytic activation of human cathepsin K. *The Journal of Biological Chemistry*, 272(21), 13955–13960. <https://doi.org/10.1074/JBC.272.21.13955>
- Mortier, G. R., et al. (2019). Nosology and classification of genetic skeletal disorders: 2019 revision. *American Journal of Medical Genetics Part*, 179(12), 2393–2419. <https://doi.org/10.1002/AJMG.A.61366>
- Polymeropoulos, M. H., Ortiz de Luna, R. I., Ide, S. E., Torres, R., Rubenstein, J., & Francomano, C. A. (1995). The gene for pycnodysostosis maps to human chromosome 1cen-q21. *Nature Genetics*, 10(2), 238–239. <https://doi.org/10.1038/NG0695-238>
- Schmidt, G. S., Schacht, J. P., Knee, T. S., Shakir, M. K. M., & Hoang, T. D. (2020). Pycnodysostosis (osteopetrosis acro-osteolytica).

- AACE Clinical Case Reports*, 6(5), e257–e261. <https://doi.org/10.4158/ACCR-2020-0169>
- Sedano, H. D., Gorlin, R. J., & Anderson, V. E. (1968). Pycnodysostosis. Clinical and genetic considerations. *American Journal of Diseases of Children*, 116(1), 70–77. <https://doi.org/10.1001/ARCHPEDI.1968.02100020072010>
- Simpson, M. A., Irving, M. D., Asilmaz, E., Gray, M. J., Dafou, D., Elmslie, F. V., Mansour, S., Holder, S. E., Brain, C. E., Burton, B. K., Kim, K. H., Pauli, R. M., Aftimos, S., Stewart, H., Kim, C. A., Holder-Espinasse, M., Robertson, S. P., Drake, W. M., & Trembath, R. C. (2011). Mutations in NOTCH2 cause Hajdu-Cheney syndrome, a disorder of severe and progressive bone loss. *Nature genetics*, 43(4), 303–305. <https://doi.org/10.1038/NG.779>
- Stenson, P. D., Ball, E. V., Mort, M., Phillips, A. D., Shiel, J. A., Thomas, N. S. T., Abeyasinghe, S., Krawczak, M., & Cooper, D. N. (2003). Human gene mutation database (HGMD): 2003 update. *Human Mutation*, 21(6), 577–581. <https://doi.org/10.1002/HUMU.10212>
- The WHO Child Growth Standards. XXXXXX n.d. <https://www.who.int/tools/child-growth-standards/standards>
- Xue, Y., Cai, T., Shi, S., Wang, W., Zhang, Y., Mao, T., & Duan, X. (2011). Clinical and animal research findings in pycnodysostosis and gene mutations of cathepsin K from 1996 to 2011. *Orphanet Journal of Rare Diseases*, 6(1), 20. <https://doi.org/10.1186/1750-1172-6-20>

How to cite this article: Markova, T. V., Kenis, V., Melchenko, E., Guseva, D., Osipova, D., Galeeva, N., Nagornova, T. & Dadali, E. L. (2022). Clinical and genetic characterization of three Russian patients with pycnodysostosis due to pathogenic variants in the CTSK gene. *Molecular Genetics & Genomic Medicine*, 10, e1904. <https://doi.org/10.1002/mgg3.1904>